Study of Ne- and Ni-like x-ray lasers using the prepulse technique

Yuelin Li,[a] Georg Pretzler, Peixiang Lu,[a] and Ernst E. Fill
Max-Planck-Institut für Quantenoptik, D-85748, Garching, Germany

Joseph Nilsen
Lawrence Livermore National Laboratory, Livermore, California 94550

(Received 13 February 1996; accepted 1 October 1996)

Recent studies of lasing in Ne- and Ni-like ions on the Asterix IV iodine laser [H. Baumhacker *et al.* Appl. Phys. B **61**, 325 (1995)] using the prepulse technique are reviewed. Experimental evidence shows that beam refraction is the main factor for the lack of lasing in low-Z elements, as well as the $J=0-1$ vs $J=2-1$ anomaly in Ne-like ion lasers when there is no prepulse. It is shown that the role of the prepulse in enhancing the $J=0-1$ lasing line in Ne-like ion is to produce a larger and more homogeneous plasma. The measurement of lasing on the $J=0-1$, $3p-3s$ transition in Ne-like Mn, V, Sc, Ca, K, Cl, S, and Si using the prepulse technique is reviewed. Wavelengths of these lasers range from 22 to 87 nm with gain lengths between 7 and 12. The drive energy for S was scaled down to 20 J. The experiment demonstrating the 12 nm lasing on the $J=0-1$, $4d-4p$ transition in Ni-like Sn is also reviewed.
[S1070-664X(97)01301-3]

I. INTRODUCTION

Although the initial prediction of Ne-like ion lasing was mainly for elements with Z around and lower than 20 on the $3p^1S_0-3s^1P_1$ transition (commonly referred to as the $J=0-1$ laser line),[1,2] the first successful demonstration of a Ne-like ion laser was in Se on the $3p^1D_2-3s^3P_1$ and $3p^3P_2-3s^1P_1$ transitions (commonly referred to as the $J=2-1$ laser lines) at 20.6 and 20.9 nm,[3,4] the atomic number of which is 34. (Because we are mainly interested in low-Z elements, the notation of LS coupling is used.) Since then, a dominant effort has been to use high Z elements to achieve lasing at shorter wavelengths.[5–8] In these experiments, mainly at Lawrence Livermore National Laboratory, exploding foil targets were used to mitigate the effects of refraction of the x-ray laser beams as they propagate down the amplifier.[3] Efforts at other institutions on smaller facilities have resulted in the demonstration of lasing in Ge, Zn, and Cu using slab targets,[9,10] among which Ge has thereafter been studied worldwide under a variety of pump conditions.[11–14] For a number of elements saturated output was obtained.[12,13,15,16] For the analogous transitions in Ni-like ions,[17–22] lasing at a wavelength as short as 3.6 nm in Au has been achieved.[15] Importantly, Ni-like ions lase dominantly on the $J=0-1,4d-4p$ transitions, in contrast to Ne-like lasers in which the $J=0-1$ laser line, which was predicted to be most amplified,[1–3] is missing or shows only very low gain in comparison with the $J=2-1$ laser lines. This is the so-called $J=0-1$ anomaly in Ne-like lasers.

This so-called $J=0-1$ anomaly is now solved by using the prepulse technique,[23–25] curved targets,[26–28] and multiple pulse irradiation,[28–30] which dramatically enhanced the brightness of the $J=0-1$ line relative to the $J=2-1$ lines in Ne-like Cu ($Z=29$) to Se ($Z=34$).[23,27–36]

In particular, application of the prepulse technique has readily made the $J=0-1$ line lase in Ni ($Z=28$) to Si ($Z=14$).[23–25,36–40] This provides an efficient way towards a small scale system using low-Z materials lasing in the soft x-ray (SXR) and extreme ultraviolet (XUV) region. Lasing in this region has long been missing[41] until the demonstration of a table top laser at 46.9 nm in Ne-like Ar using a capillary discharge,[42] and a 10 Hz optical field ionizing 41.8 nm laser in Pd-like Xe.[43] This attempt of going to low-Z elements is different from previous work, where while the lasing wavelength becomes shorter and shorter, the drive demand becomes higher and higher.

In this paper, we review in detail recent works of the x-ray laser group at the Max-Planck-Institut für Quantenoptik (MPQ), concentrating on collisional x-ray lasers using the prepulse technique. All these works are accomplished on the Asterix iodine laser.[44] Under a typical condition, Asterix was operated at 1.315 μm with a pulse duration [full width at half maximum (FWHM)] of 450 ps. The methods of generating the line focus, 3 cm long and 150 μm wide, and the well-defined prepulse are described in Ref. 34. With 400 J of Asterix output, the irradiance on the target is 2×10^{13} W cm^{-2}. Unless specified, the prepulse-to-main pulse delay was 5.23 ns. The setup of the diagnostics can be found in Refs. 34 and 37. Briefly, two on-axis transmission grating spectrometers were employed. One of them was coupled to a thinned, backside illuminated charge coupled device (CCD)[45] with either angular or spatial resolution normal to the target surface. The other spectrometer was coupled to an x-ray streak camera.[46] Experiments have been performed for both better understanding of the physics of x-ray lasers as well as extending the availability of them.

Section II will review experimental results that directly illustrate the role of beam refraction in dictating the $J=0-1$ anomaly, and in the difficulty of demonstrating a low-Z Ne-like x-ray laser. Section III gives results showing the role of the prepulse in enhancing the $J=0-1$ laser in Ne-like ions. Sections IV and V review our efforts of extending the Ne-like and Ni-like laser schemes to low-Z materials.

[a]Permanent address: Shanghai Institute of Optics and Fine Mechanics, P.O. Box 800-211, Shanghai 201800, People's Republic of China.

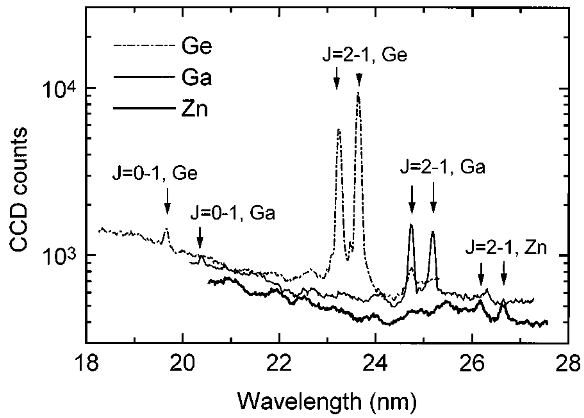

FIG. 1. Traces at the spatial maxima of the time integrated but spatially resolved on-axis spectra from 2.4 cm targets of Ge, Ga, and Zn slab targets. For these shots, Asterix irradiated the slab targets with 400 ± 20 J without any prepulse.

II. EFFECTS OF REFRACTION ON THE OUTPUT OF NE-LIKE LASERS

It is well known that Ge is a very reliable lasing material with drive wavelengths ranging from 1.315 to 0.53 μm.[9–14] However, in spite of the minor difference between the atomic numbers of Zn and Ge, in Zn only marginal lasing has been reported for drive wavelengths at 1.315 and 1.06 μm if *no prepulse* is applied.[10,34] Below Zn, Cu is the only lasing element *without* the use of the prepulse technique.[10] To understand these observations, we compared the lasing output of Ge, Ga, and Zn under similar conditions *without a prepulse*.[35] The result is illustrated in Fig. 1, where the traces at the spatial maxima of the time integrated but spatially resolved on-axis spectra from 2.4 cm targets are given. For these shots, the Asterix laser was used to irradiate slab targets with 400 ± 20 J of energy without any prepulse. One clearly sees the $J=0-1$ line at 19.6 nm and the pair of $J=2-1$ lines at 23.2 and 23.6 nm in Ge, the pair of $J=2-1$ lines at 24.7 and 25.1 nm in Ga. In Zn, even the pair of $J=2-1$ lines at 26.2 and 26.7 nm are only barely seen.

In connection with the observation that the three materials lase well with a prepulse, we ascribe the phenomenon in Fig. 1 to the effect of refraction of the x-ray laser beams. Because Zn needs a lower density to lase in comparison with Ge and Ga, it lases farthest from the target surface (for relevant scaling laws for the optimum electron density as a function of Z, see Refs. 5, 47, 48, and below). Therefore a density profile that can explain the observation in Fig. 1 by refraction effects should be such that the farther from the target the larger the density gradient. This is obviously different from the sonic rarefaction wave in the case of an isothermal steady state where the density profile is exponential.[49] At the time when the gain peaks, such steepened plasma front is normally observed in numerical simulations, e.g., in Refs. 24 and 47. From the calculation in Ref. 47 (no prepulse), the gain region for the $J=0-1$ line in Fe, Ti, and S is shown to be farther and farther from the target and its spatial width is narrower and narrower as one goes from Fe to S due to this steepened density profile. We ascribed this steepened density profile to the unsteady nature of the early expansion of the plasma. Two reasons may lead to such a steepened density profile: (1) If the plasma is supersonic at the critical surface, a steep plasma front exists;[50] (2) When a spatially isothermal plasma expands with a rising temperature the density profile is steepened, and the faster the temperature increases, the steeper the density profile is.[51] This hydrodynamic motion in combination with the beam refraction is clearly the reason that no laser in lower-Z Ne-like ion can be observed without modifying the hydrodynamics or compensating the refraction. More detailed and quantitative modeling, especially the effect of beam refraction, would be necessary for better understanding the observation.

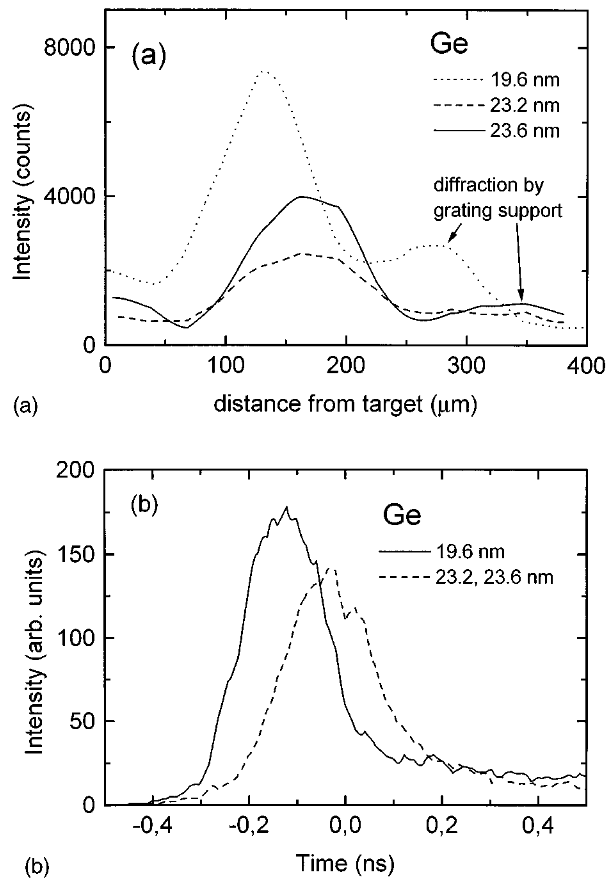

FIG. 2. The spatial distribution (a) and time history (b) of the $J=0-1$ line at 19.6 nm and the pair of $J=2-1$ lines at 23.2 and 23.6 nm in Ge. A 1.2 cm target was used for the measurement in (a) and a 2.5 cm target was used for (b), (b) was measured at 7 mrad off axis, where the angular maximum of the 19.6 nm line appears. For both cases, a 420 J drive pulse with an 8 J prepulse was used. For (a), the accuracy of determining the target surface position is ±50 μm. In (b) the time zero is set at the peak of the continuum emission, which approximately corresponds to the peak of the drive pulse. The pair of $J=2-1$ lines are not resolved in (b) due to the low spectral resolution of the spectrometer.

To show the origin of the $J=0-1$ anomaly, we give in Fig. 2 the spatial distribution (a) and time history (b) of the $J=0-1$ and the pair of $J=2-1$ lines in Ge. A 1.2 cm target was used for the measurement in Fig. 2(a) and a 2.5 cm target was used for a better signal-to-noise ratio for Fig. 2(b), respectively. For both cases, a 380 J drive pulse with a 7 J prepulse was used. The $J=0-1$ line is seen to occur closer to the target surface and earlier in time, which readily explains the $J=0-1$ anomaly: the propagation of the $J=0-1$ laser is more subjected to refraction effects. It is also experimentally observed that the $J=0-1$ line is more affected by refraction than the $J=2-1$ lines using an angular resolved measurement *without* a prepulse.[10] These observations in Fig. 2 are in good qualitative agreement with hydrodynamic and atomic kinetic modeling.[52]

Physically, this originates from the fact that the $J=0-1$ line is predominately pumped by direct monopole excitation from the Ne-like ground state[1,2] while the $J=2-1$ lines are more influenced by recombination from F-like ions and cascading from higher levels.[53,54] In this case pumping of the $J=0-1$ line relies more on a high electron density and high abundance of the ground state. As the plasma is stripped rapidly through Ne-like stage, lasing on the $J=0-1$ line can only occur early in time, and is more transient than that on the $J=2-1$ lines.

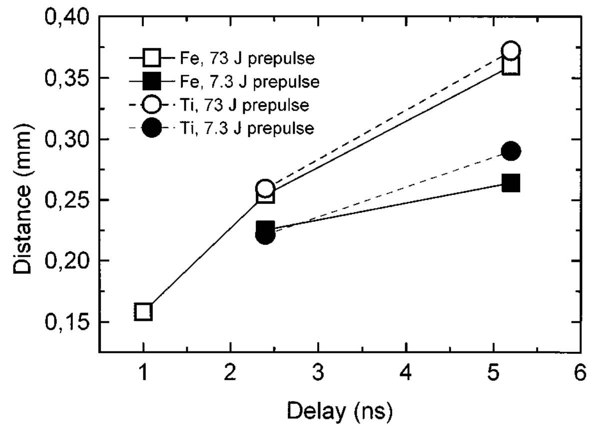

FIG. 4. The peak positions of the $J=0-1$ line in Fe and Ti as a function of the prepulse-to-main pulse delay at 7.3 and 73 J prepulse levels with a main pulse energy of 417 J. The target length is 1.2 cm.

III. THE EFFECT OF THE PREPULSE

Both in our experiments and in the literature, it is now a routine observation that the prepulse is essential in enhancing the $J=0-1$ line. For instance, in Ga, with a main pulse energy of 380 J, effective gains of 4.3, 3.1, and 2.8 cm^{-1} for the $J=0-1$ and the pair of $J=2-1$ lines have been measured for the case with a 70 J prepulse, as compared to the gains of 0, 2, and 2 cm^{-1} in the case of no prepulse.[35] The low-Z elements ($Z<29$) do not lase at all without a prepulse.

To understand the role of the prepulse in making this dramatic change, a series of experiments measuring the spatial profile of the laser output has been performed.[52,55,56] A detailed investigation of the Z dependence at a 5.23 ns delay and two prepulse levels was described in Ref. 55, where the results were interpreted assuming a power law for the optimal electron density and an adiabatic similarity expansion of the preplasma: briefly, a lower Z element needs a lower optimum electron density, and a larger prepulse produces a plasma expanding faster, therefore the lower the Z and the larger the prepulse, the further the gain region is from the target surface. Our spatially resolved measurements for the lasing position were compared with hydrodynamic and atomic kinetic modeling and good qualitative agreements were observed.[52,56] To further illustrate this point, in Fig. 3, we present the spatial distributions as a function of the prepulse-main pulse delay for the $J=0-1$, 25.5 nm laser in Fe. The delays used are 1, 2.3, and 5.23 ns, and the main pulse energy is 417 J, with 7.3 or 73 J prepulses. In these measurements, the target lengths were 1.2 cm. In Fig. 4 the peak positions of the $J=0-1$ line in Fe and Ti are plotted as a function of the delay at 7.3 and 73 prepulses. Clearly a longer delay shifts the lasing region farther away from the target surface. Another direct illustration of the effect of the prepulse is the reduced refractive angle but increased beam divergence of the output laser beam in comparison with the case of no prepulse, as shown in Fig. 5 for the 23.6 nm $J=2-1$ line in Ge. The larger beam divergence when using a prepulse is due to the broader gain region, and the reduced refraction angle is the effect of the relaxed plasma density gradient.

These observations verified that the key role of the prepulse is to produce a plasma with a longer scale length,

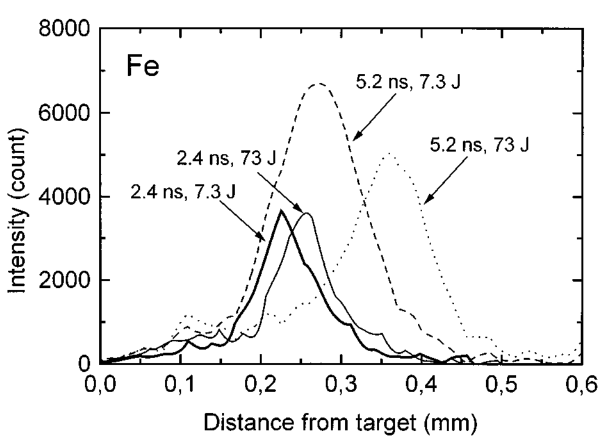

FIG. 3. The spatial distribution of the $J=0-1$, 25.5 nm laser in Fe for a main pulse energy of 417 J with 7.3 and 73 J prepulses, at 2.3 and 5.23 ns delays. The target lengths were 1.2 cm. The position at 0 is determined to be accurate within ± 50 μm.

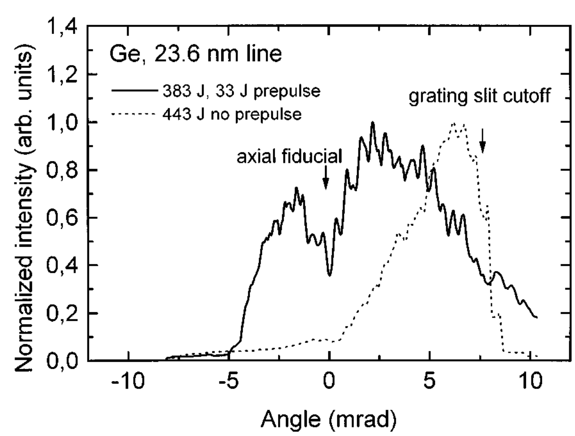

FIG. 5. Angular profiles in the horizontal plane of the $J=2-1$ line at 23.6 nm in Ge with and without a prepulse. The target lengths were 2.5 cm.

thus allowing a better propagation of the x-ray laser beam. Simulation in Ref. 57, additionally, indicates that a longer scale length (as the result of a larger prepulse or a longer prepulse-to-main pulse delay) results in a better coupling of the main pulse energy while reducing the hydrodynamic losses during the irradiation.

An important point is the dependence of the lasing output on the prepulse level. First, as a higher electron temperature results in a higher gain, a small amount of the plasma, i.e., a smaller prepulse, is preferred for a higher gain. However, this high gain may not be effective if the beam refraction dominates the propagation when the scale length of the plasma is too short. Simple analysis shows (see Appendix A), that the optimized prepulse is a function of the target length as well as of the lasing materials, which is consistent with simulations of Ref. 57. Experimental results about the optimization of the prepulse can be found in Refs. 35, 39, 55, 58, and 59.

IV. LOW-*Z* Ne-LIKE LASERS USING THE PREPULSE TECHNIQUE

Analysis based on a four-level model reveals that for elements with Z between 32 and 14, the electron temperature (T_e), the optimum electron density (n_{opt}), and the gain coefficient (G) of the $J=0-1$ laser in Ne-like ions follow the scaling[48]

$$T_e \sim (Z-6.4)^{1.9}, n_{\mathrm{opt}} \sim (Z-8.8)^{6.1}, G \sim (Z-7.0)^{2.7}.$$

Predictions of these scaling laws are quite favorable for low-Z materials. First, the decreased temperature required reduces the drive demand. Second, the gain coefficient drops only moderately as Z decreases. The main factor affecting lasing in these low-Z materials is the low electron density required. In Refs. 42 and 43 this requirement was met by using gases as lasing media.

The prepulse technique makes it possible to create a low density plasma. Using this technique we have demonstrated lasing on the $J=0-1$ transition in Ne-like Ga ($Z=31$),[35] Mn($Z=25$),[40] V ($Z=23$),[37] Sc, Ca, K, Cl ($Z=21,20,19$, and 17),[38] S and Si ($Z=16$ and 14).[39] These lasers were demonstrated with main pulse energies ranging from 420 to 20 J, preceded by prepulses with energies from 70 to 0.4 J. We mention that lasing on the same transition in Ne-like Ar ($Z=18$) has also been demonstrated in a laser irradiated gas puff target without the use of a prepulse.[60] The wavelengths[61] and the gain coefficients obtained in our experiments are listed in Table I. For targets, CaF_2 and KCl, LiCl crystals were used for Ca, K, Cl; for S, fine powders were glued on a glass substrate. The other targets were slabs thicker than 100 μm.

A. General observations

In spectra of these lasers, the normal $J=0-1$ lasing line, i.e., the $3p^1S_0-3s^1P_1$ transition (the analogue of the 19.6 nm line in Ge and 18.2 nm line in Se, termed E line in Ref. 61) dominates the spectra. We note that it is the failure in observing lasing in V and Sc has initially led the authors of Ref. 23 to the speculation that the E line at 32.6 nm in Ti is resonantly photopumed, although gain on this line has been predicted owing to the strong $2p-3p$ monopole excitation.[1,2]

For the pure (noncompound) target cases, the E lines at 26.9, 28.5, 30.4, 32.6, and 35.3 nm in Mn, Cr, V, Ti, and Sc ($Z=25$, 24, 23, 22, and 21) were observed to be weaker in odd-Z elements than in even-Z elements. Under conditions listed in Table I with target lengths of about 2.5 cm, they are of relative intensities of 56, 665, 86, 8, and 42 thousand CCD counts for Mn, Cr, V, Ti, and Sc, respectively.[40] This is consistent with the hyperfine splitting effect due to the nonzero nuclear spin in odd-Z elements, which reduces the gain on the E line by effectively increasing the linewidth.[62,63]

In these elements, we also observed a second $J=0-1$ line, which are at 22.1, 23.9, 26.1, 28.4, and 31.2 nm in Mn, Cr, V, Ti, and Sc. They are identified as the $3p$ $^1S_0-3s^3P_1$ transition (termed G transition in Ref. 61). In the similar shots mentioned above, the intensity of the G line is less than 2 thousand CCD counts except for the 26.1 nm line in V, which has an intensity of 15 thousand CCD counts.[40] The weaker G line in Mn, Cr, Ti, and Sc is in consistency with previous observations in Fe, Co, and Ni,[36,56] which is due to the fact that the G line shares a common upper level with the E line but has a smaller oscil-

TABLE I. Transitions, wavelengths (λ), gain coefficients (g), and gain lengths (gl) for the new Ne-like lasing observed. An error bar of ± 0.8 cm^{-1} applies when error is not given, mainly due to the shot-to-shot deviation. The energies of main pulse (prepulse) under which the gain was measured are also given. When not specified, pure (noncompound) slab targets were used. Gain coefficients deduced using the method of Appendix B are also given for V and Sc in brackets, which are used for the gain ratios shown in Fig. 6 [for lasing in Ne-like Si, the gain coefficient has not been measured due to lack of data at different target lengths (see Ref. 39)].

Ions (targets)	Terms	λ(nm)	E(J)	g (cm^{-1})	gl	References
Ga^{21+}	E [a]	20.4	380 (70)	4.3	10.7	Ref. 35
	A [b]	24.7		3.1	7.4	
	B [c]	25.1		2.8	6.7	
Mn^{15+}	E	26.9	370 (66)	4.3	10.7	Ref. 40
	G [d]	22.1		2.5	6.3	
V^{13+}	E	30.4	370 (66)	4.4±0.7 (3.7)	11.0	Ref. 37
	G	26.1		5.0±1.1(4.0)	12.5	
Sc^{11+}	E	35.2	370 (66)	3.8(4.7)	9.8	Ref. 38
	G	31.2		(2.7)		
Ca^{20+}(CaF_2)	E	38.3	370 (66)	3.8	11.4	Ref. 38
K^{9+} (Kcl)	E	42.1	370 (66)	3.4	10.2	Ref. 38
Cl^{7+} (Kcl)	E	52.9	370 (66)	2.5	7.5	Ref. 38
S^{6+}	E	60.8	420 (70)	1.5	4.5	Ref. 39
	P [e]	60.1		1.7	5.1	
Si^{4+}	E	87.4	58 (1)			Ref. 39

[a] $3p^1S_0-3s^1P_1$ transition.
[b] $3p^1D_2-3s^3P_1$ transition.
[c] $3p^3P_2-3s^1P_1$ transition.
[d] $3p^1S_0-3s^3P_1$ transition.
[e] $3d^1D_1-3p^1P_1$ transition.

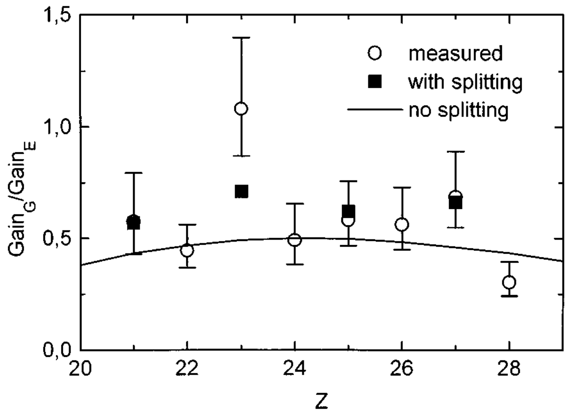

FIG. 6. Calculated and measured gain ratio of the G line to the E line as a function of atomic number. Solid line: gain ratios assuming similar population inversions for the E and G lines without hyperfine splitting. The atomic parameters in Ref. 61 are used for the calculation. When hyperfine splitting effect is included (solid squares) the gain reductions on the E line calculated in Ref. 63, i.e., 0.76, 0.69, 0.81, and 0.69 for Sc, V, Mn, and Co at ion temperatures of 43, 65, 95, and 132 eV, respectively, are used.

lator strength.[61] The hyperfine splitting has little effect on the G line.[63] However, in V, this G line (15 thousand counts) is even stronger than the E line (8 thousand counts) at 30.4 nm.[37,40] We also observed that the G line has a temporal behavior similar to that of the E line in Cr and Ti, while the E line has a much shorter duration.[40] This makes V to be very different from the other elements.

This anomalous behavior of V is clearly illustrated in Fig. 6, where the calculated and measured gain ratio of the G line to the E line is plotted as a function of the atomic number. For the G line, we were not able to measure the gain in most of the elements because it was too weak in the shorter target shots. Therefore the gain coefficients are deduced using a method described in Appendix B. In this case, for consistency of comparison, gains on the E line used are also deduced this way. For Cr, Ti, V, and Sc, the gains in Mn[40] are used as a reference. The choice of Mn is due to the fact that the measured value fits closely to the calculated tendency (see Fig. 6). For Ni and Co, the Fe result is used as reference[56] because it is the only element with a measured gain on the G line under the conditions these data were taken, i.e., with a 420 J main pulse and a 7 J prepulse. The calculated gain ratios are obtained assuming similar population inversion for both transitions using the atomic parameters in Ref. 61. When hyperfine splitting effect is considered, the gain reduction factors on the E line in Ref. 63 are applied, i.e., 0.76, 0.69, 0.81, and 0.69 for Sc, V, Mn, and Co at ion temperatures of 43, 65, 95, and 132 eV, respectively. We note that these ion temperatures in Ref. 63 are obtained from simulations for slab targets irradiated by a single 600 ps drive pulse with a strength to produce the Ne-like stage. In our case with the prepulse technique, the ion temperature might be somewhat lower due to the cooling before the main pulse arrives. Nevertheless, the measured data agree with the calculation approximately for most of the elements except for V, which is the only one that exhibits a gain ratio (G/E) exceeding 1, and deviates quite far from the calculation. This indicates that there must be other reasons that contribute to the anomalous observation in V besides the hyperfine splitting effect. As the two lines share a common upper level, a full understanding of this V anomaly would require accurate measurements of the $3-3$, and $3-2$ transition arrays in Ne-like or higher ionization stages to find possible resonance to the lasing lines or the $3s-2p$ transitions (responsible for evacuating the lower lasing level in the Ne-like ion). A resonance to the former will enhance the laser while a resonance to the latter will deplete the gain.

In S spectra at high pump energy, beside the E-line at 60.8 nm, we also observed a second laser line at 60.1 nm,[39] which is identified as the $3d^1P_1-3p^1P_1$ transition in Ne-like S, the analog of the 45.1 nm line observed in Ne-like Ar.[60,64] Lasing on this transition is tentatively attributed to trapping of the strong $3d^1P_1-2p^1S_0$ resonant radiation, while the lower lasing level is evacuated by collisions between adjacent levels.[64] For S, the gain coefficient on this line was measured to be slightly higher than that on the E line at 60.8 nm.[39] A more detailed analysis of this novel lasing system can be found in Ref. 65.

In our experiment, the strong laser lines were normally observed to be accompanied by regular wings (e.g., see figures in Refs. 38–40), which are due to diffraction by the slit on top of the transmission grating. Such patterns provide a rough estimate of the spatial coherence of the laser beam. Analysis of the pattern formed by the E line at 28.5 nm in Cr reveals that the coherence of the laser beam is not better than that of a quasimonochromatic spatially incoherent disk source whose diameter is of the order of the size of the laser output end. This is a result similar to previous measurements for the 20.6 and 20.9 nm lines in Se,[66] and the 23.2 and 23.6 nm lines in Ge.[67,68] It should be possible to greatly increase the coherence by using the injector-amplifier geometry.[12,13]

The features with respect to pulse duration, angular characteristics of the $J=0-1$ laser, are also examined.[69] Under a condition of 340 J main pulse preceded by a 60 J prepulse, the pulse duration varies gradually from 250 to 350 ps in going from Ni to S. Lasing occurs 200–300 ps before the peak of the drive pulse. The angular beam maximum was found to be insensitive to the prepulse level and the working material and was at 3–5 mrad, with a beam divergence between 5 and 10 mrad.

B. Experiments with reduced drive energy

One of our efforts is to scale down the drive energy to demonstrate the possibility of using the prepulse technique for a practically available small scale system. Previously, the $J=0-1$, 38.3 nm line in Ca lased at 100 J energy drive energy;[38] the analog in Ti at 32.6 nm has been demonstrated at 50 and 40 J drive energies.[58,59] More recently, pump energy for the $J=0-1$, 60.8 nm line in S was scaled down to an energy as low as 20 J, corresponding to a drive power of only 10^{12} W cm^{-2}.[39] The prepulse energy was only 0.36 J in this case. A typical spectrum taken under this condition is given in Fig. 7, where the 60.8 nm laser line dominates. Figure 8 depicts the peak intensity of the 60.8 nm line in S as a function of the main pulse energy at different prepulse levels for 3-cm-long targets. One notices that at a large

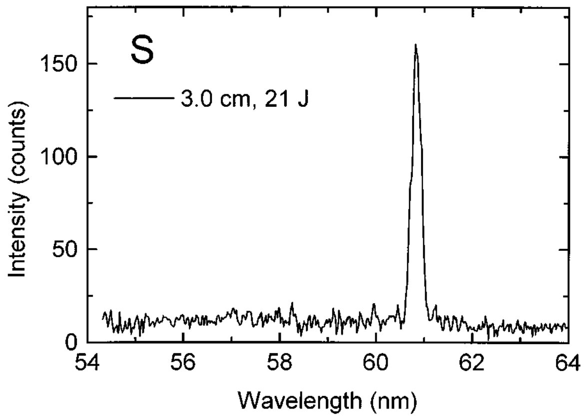

FIG. 7. A trace at the spatial maximum of the time integrated, spatially resolved spectrum from a 3 cm S target using a 20 J main pulse with a 0.36 J prepulse.

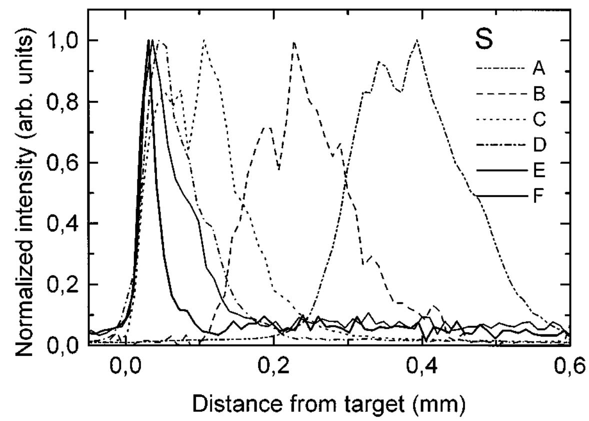

FIG. 9. Spatial distribution of the 60.8 nm laser line in S for a large range of prepulse (main pulse) energy for 3-cm-long targets: A: 70 J (430 J), B: 12.8 J (69.7 J), C: 1.0 J (59.5 J), D: 0.36 J (40.9 J), E: 0.17 J and (21 J), and F: 0.17 J (21 J), a target with 1 m radius of curvature.

prepulse of about 70 J, a reduction of the main pulse energy leads to successive reduction of the intensity of the laser line, which is a logical result due to the reduced electron temperature (note the log scale of the intensity). However, in the more interesting regime of a smaller main pulse energy at lower prepulse levels, a very different behavior is observed. For instance, for the 0.36 J prepulse, a 40 J main pulse optimizes the intensity of the laser line. Also, for a main pulse energy between 60 and 100 J, a prepulse energy of $\sim$1.0 J optimized the lasing intensity. This indicates that at low drive energies the intensity of the laser line becomes more sensitive to the prepulse level.

To understand the behavior of the 60.8 nm laser line under very small prepulses, we give the spatial profile of the laser line obtained using the spatially resolved spectrometer in Fig. 9. It is obvious that as the prepulse energy is reduced, the laser line peaks closer to the target surface, an observation similar to our previous ones. For large main pulse energies, there are some large scale modulations of the profile, which disappear as the main pulse energy is reduced. These modulation may result from the spatial profile of the neon-like ion abundance, which has been observed in simulations.[14] Finally, as the prepulse energy is reduced below 1 J, the laser line peaks almost on the target surface (the rear side slope of the profile is due to the limited spatial resolution of the spectrometer) and exhibits a very narrow profile with FWHM of about 100 μm. This is an important indication that the laser beam is not seriously affected by the refraction effect at very low prepulse levels. This is further verified by use of a target with a radius of curvature of 1 m, in which the spatial profile was further narrowed to about 40 μm while the output signal remains the same to a similar shot on a flat target. The narrowed near field profile when using a curved target is in consistence with the prediction of the ray tracing calculation.[70] It is plausible that this ''refraction free'' profile originates from the hydrodynamics of the plasma when the main pulse arrives. The tenuous preplasma produced by the tiny prepulse allows the main pulse to heat the solid target and produce new plasmas that interact with the preplasma. This interaction may lead to ripples in the density profile, which in turn establish low density channels in the plasma that guide the x-ray laser beam along the target surface. Such ripples have been observed in the simulation at low prepulse levels and disappear at larger prepulses.[57] Further theoretical and numerical investigation is needed to quantitatively understand the laser plasma interactions in this regime and the relevant beam refraction in such lasant plasmas.

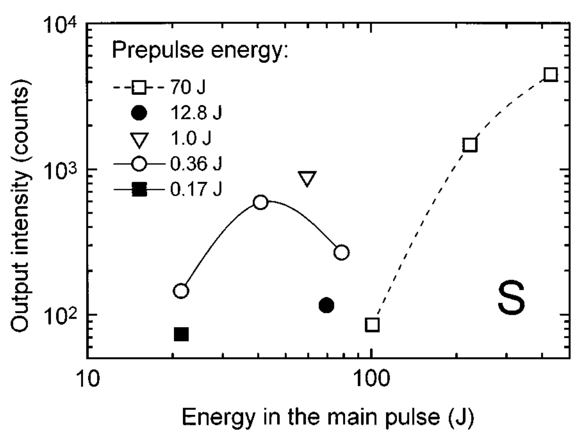

FIG. 8. The peak intensity of the 60.8 nm E line in S as a function of the main pulse energy at different prepulse levels for 3-cm-long targets.

V. SCALING TO SHORTER WAVELENGTHS: Ni-LIKE Sn LASER AT 12 nm

The Ne-like lasers described above emit at rather long wavelengths. To scale to short wavelengths, an obvious way is to use the Ni-like scheme,[15,17–22] for which a small scale system in low-Z elements has been proposed[71] and initially studied experimentally.[72,73] More recently, using a multiple pulse irradiation technique lasing in a number of middle-Z elements has been demonstrated at considerably lower drive energy[74,75] than those in these previous experiments.[20–22]

To go to short wavelengths using low-Z Ni-like ions, we did a series of experiments and succeeded in demonstrating lasing at 12 nm in Ni-like Sn with a gain length of about

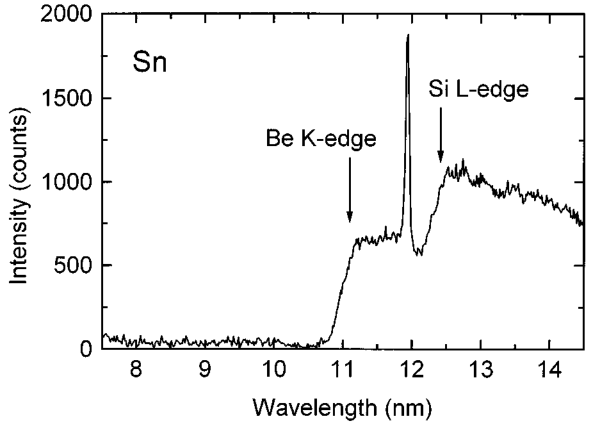

FIG. 10. A trace at the spatial maximum of the time integrated, spatially resolved spectrum from a 3-cm-long curved target of Sn, the radius of curvature of which was 1 m, obtained with a 442 J main pulse preceded by a 39 J prepulse. A strong laser on the Ni-like $J=0-1$, $3d_{3/2}-3d_{5/2}4p_{3/2}$ transition, at 11.98 nm is seen. A 1 μm Be filter was used.

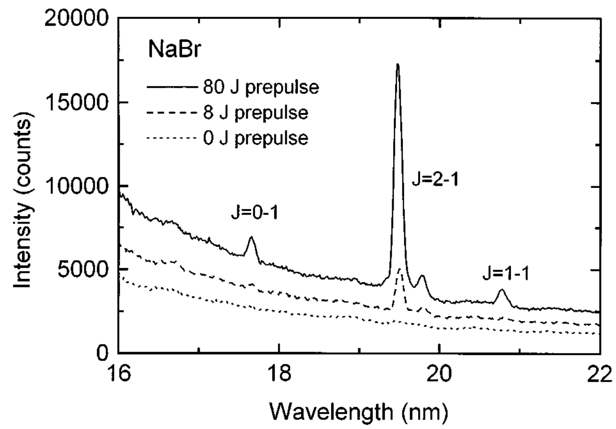

FIG. 11. Traces at the spatial maximum of the time integrated, spatially resolved spectra from 2.5-cm-long NaBr targets at a 460 J main pulse with 0, 8, and 80 J prepulse.

4.8.[76] A spectrum from a 3-cm-long curved target of Sn, the radius of curvature (termed R_t hereafter) of which was 1 m, is shown in Fig. 10. It was obtained with a 442 J main pulse preceded by a 39 J prepulse. A strong laser on the Ni-like $J=0-1$, $3d_{3/2}4d_{3/2}-3d_{5/2}4p_{3/2}$ transition is seen, while its partner, the $3d_{3/2}4d_{3/2}-3d_{3/2}4p_{1/2}$ transition predicted at 11.5 nm,[77] is absent, in consistency with the previously observed Z dependence of their relative intensities.[15,74,78] Although a previous experiment[79] has shown indication of gain in Ni-like Sn, this is the first unambiguous demonstration of this first proposed Ni-like ion laser.[17]

In the experiment, it is found that both the prepulse and curved target are playing important roles. No lasing line can be identified with a 380 J main pulse alone for a 2.5 cm flat target. With the addition of a 70 J prepulse, the lasing line is weakly seen, and has a very localized emission region, which is an indication of lasing. Under the condition for the shot shown in Fig. 10, the output of the laser line increases as R_t decreases down to 1 m. We conclude that for Ni-like ion lasers, the refraction compensation is equally important as the prepulse. This is somewhat different from the case for a Ne-like laser. In a recent experiment, the effect of the prepulse on the 19.6 nm line in Ge was found to dominate the effect of the target curvature. A curved target was found to be important only for cases with tiny prepulses.[80]

One important difference between Ne-like and Ni-like ion lasers is that as one goes to low-Z materials, the former lases under steady-state calculation even in an element like Si[1,2] while the latter, e.g., in Ni-like Mo, shows no substantial gain in a steady-state calculation. The reason is that the plasma tends to be over ionized when the temperature is high enough for a significant $3d$–$4d$ excitation.[71] Therefore, it is plausible that in these experiments with prepulse or multiple pulse irradiation, the first pulse, beside creating a plasma with a relaxed density profile, also provides an environment allowing a more transient heating of the plasma, hence generating a higher gain. In this case, a fast rising edge of the optical pumping pulse is favored. Even in this case, the gain region is still quite narrow, and therefore compensating the refraction effect seems to be crucial. This is supported by comparing the results of using exploding foil targets with the results of using curved targets, e.g., for the Eu results in Ref. 20 and the Sm, Gd results in Ref. 74; for Sn results of ours and that in Ref. 79. In both cases, the prepulse (multiple pulse) technique in conjunction with the use of curved targets has resulted in higher gains. Finally, a longer wavelength drive is also found to be more advantageous if one compares the results for Ni-like Nd in Ref. 74 with that in Ref. 78. In Ref. 74 a gain coefficient of 3 cm^{-1} is observed for the $J=0-1$ line at 7.9 nm using a 1.06 μm drive with a total energy of 200 J, as compared to the gain of about $1\,\mathrm{cm}^{-1}$ in Ref. 78 for the same line using a 0.53 μm drive with a total energy of nearly 2 kJ. This is due to the fact that when the optimum electron density is low, the drive energy at a longer wavelength couples better to the plasma region with correct densities. We note that, to the best of our knowledge, no ray tracing calculation of a Ni-like system from a slab target has been published.

Obviously, to realize high gain Ni-like lasers in low-Z elements envisaged in Ref. 71, a prepulse or multiple pulse irradiation scheme at wavelengths longer than $1\,\mu$m with a short pulse duration in conjunction with curved targets would be crucial. We suggest to use a pulsed CO_2 laser at 10.6 μm for this purpose. Previous calculation[47] and our calculation using LASNEX[81] show that to create a similar environment in the plasma, a CO_2 laser needs only 10% of the energy of a laser at $1\,\mu$m, and the plasma produced is intrinsically with low electron density, well suited for low-Z Ne or Ni-like ion lasers. In addition, the hot electrons produced by long wavelength drive lasers also contribute to directly pump the upper laser levels.[82,83] In an experiment with Cu foil targets irradiated by a CO_2 laser, indication of lasing was reported for several Ne-like transitions, although the electron density for Cu needed for lasing is too high for a CO_2 laser.[84]

For the feasibility of extending the prepulse or multiple pulse technique to high-Z elements as an alternative to producing lasing at short wavelengths, results and discussions can be found in Refs. 30, 31, 85, and 86. In this context, we show in Fig. 11 a set of spectra from 2.5-cm-long NaBr targets at a 460 J main pulse with 0, 8, and 80 J prepulses. Lasing in Ne-like Br ($Z=35$) has previously been reported using an exploding foil target at a drive energy of 2 kJ.[87] In Fig. 11, the shorter wavelength $J=2-1$ line (the analogue to the 23.2 nm line in Ge) dominates due possibly to the hyperfine splitting effect, which reduces the gain on the longer wavelength line (Refs. 62, 63, and 87). To explain the weak $J=0-1$ line at 17.4 nm, besides the hyperfine effect, the electron density that can be produced by the 1.315 μm Asterix may be too low for it to be well pumped. Clearly a larger prepulse makes the laser stronger. For a ZnSe target, we also observed that the $J=0-1$ line at 18.2 nm in Se has the same intensity as the $J=2-1$ lines at 20.6 and 20.9 nm with a 425 J main pulse preceded by a 75 J prepulse, a similar observation to that in Ref. 31 at a 0.53 μm drive wavelength. Without a prepulse or with only a small prepulse, no lasing could be observed for ZnSe and NaBr targets.

VI. SUMMARY

We review our recent studies of lasing in Ne- and Ni-like ions on the Asterix IV iodine laser using the prepulse technique. We give experimental evidence that beam refraction is the main factor for the lack of demonstration of lasing in low-Z elements, as well as the $J=0-1$ vs $J=2-1$ anomaly in Ne-like ion lasers when there is no prepulse. We show that the role of the prepulse in enhancing the $J=0-1$ lasing line in Ne-like ion is to produce a larger and more homogeneous plasma. We reviewed the measurement of lasing on the $J=0-1$, $3p-3s$ transition in Ne-like Mn, V, Sc, Ca, K, Cl, S, and Si, and lasing on the $J=0-1$, $4d-4p$ transition in Ni-like Sn. The drive energy for the 60.8 nm Ne-like S laser was scaled down to 20 J. These experiments might be important evolutionary steps towards small scale SXR and XUV laser systems using laser plasma as lasing medium. First, due to the small excitation energies in these low-Z Ne- and Ni-like ions, reduction of the pump demand seems possible, as we have demonstrated for Ne-like S. Second, we showed the role of the prepulse and its effect on the laser output. Based on these results, small pump lasers at longer wavelengths (>1 μm) with output energy of no more than 50 J seem to be enough for driving these lasers using the prepulse or multiple pulse techniques.

ACKNOWLEDGMENTS

The authors would like to thank the Asterix facilities crew for providing support for the experiments.

Li was supported by the Alexander von Humboldt Foundation and, partly within the framework of the agreement between the Max-Planck Society and Academia Sinica, he thanks Dr. S. Witkowski and his colleagues at MPQ for their hospitality. Lu was supported by the Alexander von Humboldt Foundation. Pretzler was supported by the EU Program ''HCM'' No. CT920015. Nilsen's work was performed under the auspices of the U. S. Department of Energy through the Lawrence Livermore National Laboratory under Contract No. W-7405-ENG-48. This work was supported in part by the Commission of the European Communities in the framework of the Association Euratom/Max-Planck-Institut für Plasmaphysik.

APPENDIX A: SCALING OF THE OPTIMUM PREPULSE INTENSITY

To derive a scaling law for an optimum prepulse intensity, we assume a cylindrical preplasma with a linear density profile $N_e(r)=N_0(L_p-r)/L_p$, where r is the distance from the line focus and N_0 is the density at the symmetrical center. For simplicity we set $N_0\sim 1/\lambda_0^2$, being the critical density of the pump laser, with λ_0 the wavelength of the drive laser. If inverse bremsstrahlung is the mechanism for absorption of the pump laser and the plasma is spatially isothermal, one has the electron temperature as[88]

$$T_e \propto \frac{[1-\exp(-\alpha L_p)]}{N_0 L_p^2} I_{\mathrm{main}},$$

where α is related to the electron–ion collisional frequency at the critical density, I_{main} is the intensity of the main pulse. When L_p is large enough, the exponential term vanishes and T_e becomes a monotonously decreasing function of L_p. In this case, for gain production one needs

$$L_p < \beta \frac{\lambda_0 I_{\mathrm{main}}^{1/2}}{Z-6.4}, \tag{A1}$$

where the scaling of $T_e > T_{\mathrm{th}} \sim (Z-6.4)^2$ (Ref. 48) is used for lasing threshold; β is a constant related to the transverse expansion of the preplasma.

On the other hand, the refractive index of the photons is $n(r)=[1-N_e(r)/N_x]^{1/2}\approx 1-0.5N_e/N_x$, where N_x is the critical density of the x ray. From the paraxial ray equation in a medium of near-unity refractive index[3]

$$\frac{d^2r}{dy^2} = -\frac{1}{2N_x}\frac{dN_e(r)}{dr}.$$

Here y is the coordinate along the plasma column. For a linear electron density profile, the transverse deflection of a paraxial beam after traveling a target length of Y_0 is

$$\Delta r = -\frac{1}{4}\left(\frac{\lambda_x}{\lambda_0}\right)^2 \frac{Y_0^2}{L_p},$$

where λ_x is the wavelength of the x-ray laser. If only the density dependence around the optimum electron density is considered, we have Gain$\sim N_e(1-0.5N_e/N_{\mathrm{opt}})$.[48] The spatial FWHM of the gain region is

$$w_{\mathrm{Gain}} \propto \frac{N_{\mathrm{opt}}}{N_o} L_p,$$

where $N_{\mathrm{opt}}\sim(Z-8.8)^6$ is the optimal electron density for lasing.[48] Using $\Delta r \leqslant w_{\mathrm{Gain}}$, one has

$$L_p \geqslant \gamma \frac{Y_0}{(Z-8.8)^3 (Z-10)^{0.9} \lambda_0^2}, \tag{A2}$$

where γ is a constant and $\lambda_x \sim (Z-10)^{-0.9}$ for the E line is used.[48]

In the preplasma one has $L_p \sim I_p^{\kappa}$, where I_p is the intensity of the prepulse and κ is a parameter related to the laser-plasma interaction process. Therefore from Eqs. (A1) and (A2) we have

$$I_p < a\left(\frac{\lambda_0 I_{\mathrm{main}}^{1/2}}{Z-6.4}\right)^{1/\kappa},$$
$$I_p \geqslant b\left(\frac{Y_0}{(Z-8.8)^3(Z-10)^{0.9}\lambda_0^2}\right)^{1/\kappa}, \tag{A3}$$

where a and b are constants. It is obvious that the upper limit of I_p is set by the atomic number of the lasing material and the main pulse energy, whereas the lower limit is additionally related to the target length (Y_0). Though qualitatively, Eq. (A3) gives a general scaling of the optimized prepulse levels: for high-Z targets, small prepulses are favorable, and for long targets large prepulses are better. Note that the analysis is valid only for large enough prepulses so that the main pulse energy is absorbed completely by the preplasma.

APPENDIX B: A METHOD FOR GAIN MEASUREMENT

To deduce the gain (G_1) on line 1 from the known gain (G_{ref}) on a reference line in an adjacent element, let us first recall the Linford formula[89] for lasing output intensity

$$I=\frac{I_0}{G}\frac{[\exp(GL)-1]^{3/2}}{[GL\exp(GL)]^{1/2}}=I_0 f(G,L), \tag{B1}$$

where G and L are, respectively, the gain coefficient and target length, $I_0 \sim A_{\mathrm{ul}} N_u E_{\mathrm{lu}}$ (as seen by a detector) is the source function of the laser line with A_{ul} and N_u the spontaneous radiation rate and number density of the upper lasing level. As a first order approximation, near the optimum condition one has $N_u \approx N_0 C_{0u}/C_{\mathrm{ul}}$, where N_0 is the number density of the ground state, C_{0u} is the monopole excitation rate from the ground state to the upper lasing level

$$C_{0u}=\frac{2.6\times 10^{-6}}{E_{0u}T_e^{1/2}}\exp\left(-\frac{E_{0u}}{T_e}\right)\mathrm{cm}^3\ \mathrm{s}^{-1} \tag{B2}$$

and C_{ul} is the collisional de-excitation rate of the upper to the lower lasing level[90]

$$C_{\mathrm{ul}}=1.65\times 10^{-5}\frac{g_l}{g_u}\frac{f_{\mathrm{lu}}\langle g_{\mathrm{lu}}\rangle}{E_{\mathrm{lu}}T_e^{1/2}}\ \mathrm{cm}^3\ \mathrm{s}^{-1}. \tag{B3}$$

Here $\langle g_{\mathrm{lu}}\rangle$ is the Gaunt factor, f_{lu} is the oscillator strength, g_l and g_u are statistic weights, and E_{0u} and E_{lu} are the excitation energy for the Ne-like ground state and the lower lasing level to the upper lasing levels in eV, respectively. T_e is the electron temperature in eV. With $N_0 \sim N_{\mathrm{opt}}/(Z-9)$ (one can also take into account the ionization balance in a steady-state approximation with Na-, Ne-, and F-like ions, which we also found to be trivial) and the $N_{\mathrm{opt}} \sim (Z-8.8)^{6.1}(T_e/E_{0u})^{0.94}$ from Ref. 48, and $A_{\mathrm{lu}} \sim f_{\mathrm{lu}}E_{\mathrm{lu}}^2$ one has

$$I_0 \propto N_u A_{\mathrm{lu}} E_{\mathrm{lu}} \propto \frac{E_{\mathrm{lu}}^4}{E_{0u}^{1.94}}\frac{(Z-8.8)^{6.1}}{Z-9}T_e^{0.94}\exp\left(-\frac{E_{0u}}{T_e}\right). \tag{B4}$$

With the known atomic parameters,[61] the ratio of I_0 for different elements can be readily calculated. If intensity ratio I_1/I_{ref} of the two lines, and the target lengths L_1 and L_{ref} are known, from

$$\frac{I_1}{I_{\mathrm{ref}}}=\frac{I_0}{I_{0\mathrm{ref}}}\frac{f(G_1,L_1)}{f(G_{\mathrm{ref}},L_{\mathrm{ref}})} \tag{B5}$$

one can easily deduce G_1 from G_{ref}. It is found that for adjacent elements, the procedure is insensitive to T_e, because it almost cancels during the procedure.

The accuracy of this method is found to be well within the accuracy of the experiments if the intensities of the lines concerned are close to each other. The result is quite sensitive if the difference between the line intensities is large. For example, using the gain of 4.1 cm^{-1} on the E line at 25.5 nm in Fe as in Ref. 56, the gain on the E line in Ni at 23.1 nm, which was measured to be slightly stronger than its analogue in Fe, was deduced to be 4.3 cm^{-1}, being similar to the measured value from two target lengths. However, for the Fe G line at 20.5 nm, where the intensity is 100 times lower than that of the E line, the deduced gain is only 0.9 cm^{-1}, well below the measured gain of 2.3 cm^{-1}.[56] A 20% change in the reference gain leads to a 200% change in the deduced gain in this case.

The method is very useful when data are not available for directly applying the Linford formula for gain measurement. For example, for the G line in Ni, Co, Ti, and Sc, which does not appear in the short target shots.

[1] A. N. Zherikhin, K. N. Koshelev, and V. S. Letokhov, Sov. J. Quantum Electron. **6**, 82 (1976).
[2] A. V. Vinogradov, I. I. Sobel'man, and E. A. Yukov, Sov. J. Quantum Electron. **7**, 32 (1977).
[3] M. D. Rosen, P. L. Hagelstein, D. L. Matthews, E. M. Campell, A. U. Hazi, B. L. Whitten, B. J. MacGowan, R. E. Turner, and R. W. Lee, Phys. Rev. Lett. **54**, 106 (1985).
[4] D. L. Matthews, P. L. Hagelstein, M. D. Rosen, M. J. Eckart, N. M. Ceglio, A. U. Hazi, H. Medecki, B. J. MacGowan, J. E. Trebes, B. L. Whitten, E. M. Campell, C. W. Hatcher, A. M. Hawryluk, R. L. Kaufmann, L. D. Pleasance, G. Rambach, J. H. Scofield, G. Stone, and T. A. Weaver, Phys. Rev. Lett. **54**, 110 (1985).
[5] R. C. Elton, *X-Ray Lasers* (Academic, San Diego, 1990).
[6] C. J. Keane, N. M. Ceglio, B. J. MacGowan, D. L. Matthews, D. G. Nilson, J. E. Trebes, and D. A. Whelan, J. Phys. B **22**, 3343 (1989).
[7] D. J. Fields, R. S. Walling, G. M. Shimkaveg, B. J. MacGowan, L. B. Da Silva, J. H. Scofield, A. L. Osterheld, T. W. Phillips, M. D. Rosen, D. L. Matthews, W. H. Goldstein, and R. E. Stewart, Phys. Rev. A **46**, 1606 (1992).
[8] C. H. Skinner, Phys. Fluids B **3**, 2420 (1991).
[9] T. N. Lee, E. A. Mclean, and R. C. Elton, Phys. Rev. Lett. **59**, 1185 (1987).
[10] E. A. McLean, T. N. Lee, J. A. Stamper, C. K. Manka, and H. R. Griem, J. Opt. Soc. Am. B **9**, 350 (1992).
[11] D. Naccache, A. Decoster, S, Jacquemot, M. Louis-Jacquet, C. J. Keane, B. J. MacGowan, and D. L. Matthews, Phys. Rev. A **42**, 3207 (1990).
[12] A. Carillon, H. Z. Chen, P. Dhez, L. Dwivedi, J. Jacoby, P. Jaegle, G. Jamelot, J. Zhang, M. H. Key, A. Kidd, A. Klisnick, R. Kodama, J. Krishan, C. L. S. Lewis, D. Neely, P. Norreys, D. M. O'Neil, G. J. Pert, S. A. Ramsden, J. P. Raucort, G. J. Tallents, and J. Uhomoibhi, Phys. Rev. Lett. **68**, 2917 (1992).
[13] S. Wang, Y. Gu, G. Zhou, S. Yu, S. Fu, Y. Ni, J. Wu, Z. Zhou, G. Han, Z. Tao, Z. Lin, S. Wang, W. Chen, D. Fan, G. Zhang, J. Sheng, H. Peng, T. Zhang, and Y. Shao, J. Opt. Soc. Am. B **9**, 360 (1992).
[14] K. Murai, H. Shiraga, G. Yuan, H. Daido, H. Azuma, E. Miura, R. Kodama, M. Takagi, T. Kanabe, H. Takabe, Y. Kato, D. Neely, D. M. O'Neil, C. L. S. Lewis, and A. Djaoui, Opt. Soc. Am. B **11**, 2287 (1994).

[15]B. J. MacGowan, L. B. Da Silva, D. J. Fields, C. J. Keane, J. A. Koch, R. A. London, D. L. Matthews, S. Maxon, S. Mrowka, A. L. Osterheld, J. H. Scofield, G. Shimkaveg, J. E. Trebes, and R. S. Walling, Phys. Fluids B **4**, 2326 (1992).
[16]L. B. Da Silva, B. J. MacGowan, S. Mrowka, J. A. Koch, R. A. London, D. L. Matthews, and J. H. Underwood, Opt. Lett. **18**, 1174 (1993).
[17]S. Maxon, P. Hagelstein, K. Reed, and J. Scofield, J. Appl. Phys. **57**, 971 (1985).
[18]S. Maxon, P. Hagelstein, J. Scofield, and Y. Lee, J. Appl. Phys. **59**, 293 (1986).
[19]P. Hagelstein, Phys. Rev. A **34**, 874 (1986).
[20]B. J. MacGowan, S. Maxon, P. L. Hagelstein, C. J. Keane, R. A. London, D. L. Matthews, M. D. Rosen, J. H. Scofield, and D. A. Whelan, Phys. Rev. Lett. **59**, 2157 (1987).
[21]B. J. MacGowan, L. B. Da Silva, D. J. Fields, C. J. Keane, J. A. Koch, R. A. London, D. L. Matthews, S. Maxon, S. Mrowka, A. L. Osterheld, J. H. Scofield, G. M. Shimkaveg, J. E. Trebes, and R. S. Walling, Phys. Fluids B **4**, 2326 (1992).
[22]B. J. MacGowan, S. Maxon, L. B. Da Silva, D. J. Fields, C. J. Keane, D. L. Matthews, A. L. Osterheld, J. H. Scofield, G. M. Shimkaveg, and J. F. Stone, Phys. Rev. Lett. **65**, 420 (1990).
[23]T. Boehly, M. Russotto, R. S. Craxton, R. Epstein, B. Yaakobi, L. B. Da Silva, J. Nilsen, E. A. Chandler, D. J. Fields, B. J. MacGowan, D. L. Matthews, J. H. Scofield, and G. Shimkaveg, Phys. Rev. A **42**, 6962 (1990).
[24]J. Nilsen, B. J. MacGowan, L. B. Da Silva, and J. C. Moreno, Phys. Rev. A **48**, 4682 (1993).
[25]J. Nilsen, J. C. Moreno, B. J. MacGowan, and J. A. Koch, Appl. Phys. B **57**, 309 (1993).
[26]J. G. Luney, Appl. Phys. Lett. **46**, 891 (1986).
[27]R. Kodama, D. Neely, Y. Kato, H. Daido, K. Murai, G. Yuan, A. MacPhee, and C. L. S. Lewis, Phys. Rev. Lett. **73**, 3215 (1994).
[28]H. Daido, R. Kodama, K. Murai, G. Yuan, M. Takagi, Y. Kato, I. W. Choi, and C. H. Nam, Opt. Lett. **20**, 61 (1995).
[29]J. C. Moreno, J. Nilsen, and L. B. Da Silva, Opt. Commun. **110**, 585 (1994).
[30]J. Nilsen and J. C. Moreno, Phys. Rev. Lett. **74**, 3376 (1995).
[31]J. Nilsen and J. C. Moreno, Opt. Lett. **19**, 1137 (1994).
[32]B. Rus, A. Carillon, B. Gauthé, P. Goedtkindt, P. Jaeglé, G. Jamelot, A. Klisnick, A. Sureau, and P. Zeitoun, J. Opt. Soc. Am. B **11**, 564 (1994).
[33]G. F. Cairns, M. J. Lamb, C. L. S. Lewis, A. G. McPhee, D. Neely, P. Norreys, M. H. Key, C. Smith, S. B. Healy, P. B. Holden, G. J. Pert, and J. A. Ploues, in *X-Ray Laser 94*, AIP Conf. Proc. No. 332, edited by D. C. Eder and D. L. Matthews (American Institute of Physics, New York, 1994), p. 289.
[34]E. E. Fill, U. Li, D. Schlögl, J. Steingruber, and J. Nilsen, Opt. Lett. **20**, 374 (1995).
[35]E. E. Fill, Y. Li, and G. Pretzler, IEEE J. Sel. Topics Quantum Electron. **1**, 958 (1995).
[36]E. E. Fill, Y. Li, G. Pretzler, D. Schlögl, J. Steingruber, and J. Nilsen, Phys. Scr. **52**, 158 (1995).
[37]Y. Li, G. Pretzler, and E. E. Fill, Opt. Lett. **20**, 1026 (1995).
[38]Y. Li, G. Pretzler, and E. E. Fill, Phys. Rev. A **52**, R3433 (1995).
[39]Y. Li, P. Lu, G. Pretzler, and E. E. Fill, Opt. Commun. **133**, 196 (1997).
[40]Y. Li, G. Pretzler, E. E. Fill, and J. Nilsen, Appl. Phys. B **63**, 125 (1996).
[41]The result of A. A. Ilyukhin, G. V. Peregudov, E. N. Ragozin, I. I. Sobel'man, and V. A. Chirkov [JETP Lett. **25**, 535 (1977)] for Ne-like Ca is not clear due to the large uncertainty in wavelength calibration; H. Yashiro, T. Hara, K. Ando, A. Aoyagi, T. Dote, and S. Namba [in *Proceedings of the OSA Meeting on Short Wavelength Coherent Radiation: Generation and Applications*, edited by R. W. Falcone and J. Kirz (Optical Society of America, Washington, DC, 1988), p. 154] observed lasing on the $3p^3D_2 \rightarrow 3s^3P_1$ transition at 50.8 nm in Ne-like Ti, which is the analog of the 24.2 nm line in Ge, but lacked further verification.
[42]J. J. Rocca, V. Shlyapstev, F. Tomasel, O. D. Cortazar, D. Hartshorn, and J. L. A. Chilla, Phys. Rev. Lett. **73**, 2192 (1994).
[43]B. E. Lemoff, G. Y. Yin, C. L. Gordon III, C. P. J. Barty, and S. E. Harris, Phys. Rev. Lett. **74**, 1574 (1995).
[44]H. Baumhacker, G. Brederlow, E. Fill, R. Volk, S. Witkowski, and K. J. Witte, Appl. Phys. B **61**, 325 (1995).
[45]Y. Li, G. D. Tsakiris, and R. Sigel, Rev. Sci. Instrumen. **66**, 80 (1995).
[46]G. D. Tsakiris, Proc. SPIE **1032**, 910 (1989).
[47]A. V. Vinogradov and V. N. Shlyapstev, Sov. J. Quantum Electron. **13**, 1511 (1983).
[48]Y. Li and J. Nilsen, ''Analytical scaling laws for low-*Z* Ne-like lasers,'' submitted to Phys. Scr.
[49]W. M. Manheimer, D. G. Colombant, and J. H. Gardner, Phys. Fluids. **25**, 1644 (1982).
[50]R. F. Schmalz and K. Eidmann, J. Phys. Fluids **29**, 3483 (1988).
[51]E. G. Gamaly, Phys. Fluids B **5**, 944 (1993).
[52]Y. Li, G. Pretzler, E. E. Fill, and Nilsen, J. Opt. Soc. Am. B **13**, 742 (1996).
[53]B. L. Whitten, A. U. Hazi, M. H. Chen, and P. L. Hagelstein, Phys. Rev. A **33**, 3363 (1989).
[54]J. Nilsen, Phys. Scr. T **47**, 83 (1993).
[55]Y. Li, G. Pretzler, and E. E. Fill, Phys. Rev. A **51**, R4341 (1995).
[56]Y. Li, G. Pretzler, and E. E. Fill, Opt. Commun. **119**, 557 (1995).
[57]S. B. Healy, G. F. Cairns, C. L. S. Lewis, G. J. Pert, and J. A. Plowes, IEEE J. Sel. Topics Quantum Electron. **1**, 949 (1995).
[58]A. Präg, A. Glinz, J. E. Balmer, Y. Li, and E. E. Fill, Appl. Phys. B **63**, 113 (1996).
[59]J. Zhang, S. T. Chunyu, Y. L. You, Q. R. Zhang, S. J. Yang, W. Z. Huang, D. Y. Wu, X. Q. Zhuang, S. P. Liu, Y. Q. Cai, F. Y. Du, X. D. Yuan, X. F. Wei, Y. K. Zhao, H. S. Peng, and J. Nilsen, Phys. Rev. A **53**, 3640 (1996).
[60]H. Fiedorowicz, A. Bartnik, Y. Li, P. Lu, and E. E. Fill, Phys. Rev. Lett. **76**, 415 (1996).
[61]J. Nilsen and J. H. Scofield, Phys. Scr. **49**, 588 (1994).
[62]J. Nilsen, J. A. Koch, J. H. Scofield, B. J. MacGowan, and J. C. Moreno, Phys. Rev. Lett. **70**, 3713 (1993).
[63]J. H. Scofield and J. Nilsen, Phys. Rev. A **49**, 2381 (1994).
[64]J. Nilsen, H. Fiedorowicz, A. Bartnik, Y. Li, P. Lu, and E. E. Fill, Opt. Lett. **21**, 408 (1996).
[65]J. Nilsen, Phys. Rev. A **53**, 4539 (1996).
[66]J. E. Trebes, K. A. Nugent, S. Mrowka, R. A. London, T. W. Barbee, M. R. Carter, J. A. Koch, B. J. MacGowan, D. L. Matthews, L. B. Da Silva, G. F. Stone, and M. D. Feit, Phys. Rev. Lett. **68**, 588 (1992).
[67]C. L. S. Lewis, D. Neely, D. O'Neil, J. Uhomoibhi, G. Cairns, A. MacPhee, G. J. Tallents, J. Krishnan, L. Dwivedi, M. H. Key, P. Norreys, R. Kodama, R. E. Burge, S. Slark, M. Brown, G. J. Pert, P. Holden, M. Lightbody, S. A. Ramsden, J. Zhang, C. Smith, P. Jaegle, G. Jamelot, A. Carillon, A. Klisnick, J. P. Raucort, J. E. Trebes, M. R. Carter, S. Mrowka, and K. A. Nugent, *X-Ray Lasers 1992*, edited by E. E. Fill (Institute of Physics, Bristol, 1993), p. 23.
[68]Y. Kato, M. Yamanaka, H. Diado, H. Shiraga, H. Azuma, K. Murai, G. Yuan, E. Miura, T. Kanabe, M. Takagi, S. Nakai, C. L. S. Lewis, D. M. O'Neil, D. Neely, M. Niibe, N. Tsukamoto, and Y. Fukuda, in Ref. 67, p. 9.
[69]P. Lu, Y. Li, and E. E. Fill, Phys. Rev. A **54**, 5193 (1996).
[70]J. A. Plowes, G. J. Pert, and P. B. Holden, Opt. Commun. **116**, 260 (1995); **117**, 189 (1995).
[71]P. L. Hagelstein, in Ref. 41, p.28.
[72]S. Basu, J. G. Goodberlet, M. H. Muendel, S. Kaushik, and P. L. Hagelstein, in Ref. 67, p. 71.
[73]S. Basu, P. L. Hagelstein, J. G. Goodberlet, M. H. Muendel, and S. Kaushik, Appl. Phys. B **57**, 303 (1993).
[74]H. Daido, Y. Kato, K. Murai, S. Ninomiya, R. Kodama, G. Yuan, Y. Oshikane, M. Takagi, H. Takabe, and F. Koike, Phys. Rev. Lett. **75**, 1109 (1995).
[75]H. Daido, S. Ninomiya, T. Imani, R. Kodama, M. Takagi, Y. Kato, K. Murai, J. Zhang, Y. You, and Y. Gu, Opt. Lett. **21**, 958 (1996).
[76]Y. Li, G. Pretzler, P. Lu, and E. E. Fill, Phys. Rev. A **53**, R652 (1996).
[77]J. H. Scofield and B. J. MacGowan, Phys. Scr. **46**, 361 (1992).
[78]J. Nilsen and J. C. Moreno, Opt. Lett. **20**, 1386 (1995).
[79]G. D. Enright, J. Dunn, D. M. Villeneuve, S. Maxon, H. A. Baldis, A. L. Osterheld, B. La Fontaine, J. C. Kieffer, M. Nantel, and H. Pépin, in Ref. 67, p. 45.
[80]J. Nilsen, Y. Li, P. Lu, J. C. Moreno, and E. E. Fill, Opt. Commun. **124**, 287 (1996).
[81]G. B. Zimmerman and W. L. Kruer, Comments Plasma Phys. Controlled Fusion **11**, 51 (1975).
[82]J. P. Apruzese and J. Davis, Phys. Rev. A **28**, 3686 (1983).
[83]W. H. Goldstein and R. S. Walling, Phys. Rev. A **36**, 3482 (1987).
[84]G. D. Enright and N. H. Burnett, in Ref. 41, p. 84.

[85]L. B. Da Silva, R. A. London, B. J. MacGowan, S. Mrowka, and D. L. Matthews, Opt. Lett. **18**, 1174 (1993).
[86]S. Maxon, K. G. Estabrook, M. K. Prasad, A. L. Osterland, R. A. London, and D. C. Eder, Phys. Rev. Lett. **70**, 2285 (1993).
[87]J. Nilsen, J. L. Porter, B. J. MacGowan, L. B. Da Silva, and J. C. Moreno, J. Phys. B **26**, L243 (1993).
[88]W. L. Kruer, *The Physics of Laser Plasma Interactions* (Addison–Wesley, New York, 1988), Chap. 5.
[89]G. J. Linford, E. R. Peressini, W. R. Sooy, and M. L. Spaeth, Appl. Opt. **13**, 379 (1974).
[90]M. J. Seaton, in *Atomic and Molecular Processes*, edited by D. R. Bates (Academic, New York, 1962), pp. 374–420.